Journal of Thermal Biology 84 (2019) 357–367

Contents lists available at ScienceDirect

Journal of Thermal Biology

journal homepage: www.elsevier.com/locate/jtherbio

Effect of inspiration cycle and ventilation rate on heat exchange in human respiratory airways

Bharat Soni, Ameeya Kumar Nayak*

Department of Mathematics, Indian Institute of Technology Roorkee, Roorkee, India

ARTICLE INFO

Keywords:
Air conditioning
Multi-compartment mathematical model
Mucus layer
Respiration cycle

ABSTRACT

A transient three dimensional (3D) theoretical axisymmetric model is developed for heat exchange across the human respiratory tract during inspiration phase and applied to study the changes in the airway temperature and velocity profile for varying ventilation rates and inhalation temperatures. A multi-compartment approach is used to study the same to avoid the airway scaling problem from micro to nano scale. This analysis also includes the role of water evaporation in mucus and non perfused tissue layers and the role of capillary bed in thermal variations during respiration. The results of heat transfer in airway and mucus layer depend on the local morphological parameters. The results are compared with the case of hypothetical regular geometry to show the significance of local morphology. The location where the inhaled air gets saturated with the body core temperature is computed to estimate the saturation distance of air. The complete analysis is made for two breathing cycles with different inhalation to exhalation ratios. The results indicate that decreasing the ventilation rate and increasing the respiration cycle can avoid the deep penetration of heat into the tract and consequently tissue thermal injury can be avoided. We have also explained numerically the role of mucus layer in avoiding tissue injury in intra-thoracic airways. We have also observed a significant difference in results for high ventilation rates between the cases of actual (cast replica) and regular airway geometry. The numerical results are in good adjustment with existing experimental data and thus validate our approach.

1. Introduction

The primary function of human respiratory system is to deliver O_2 to all body cells and extract out toxic gas CO_2. Other functions include filtering, humidifying and conditioning the inhaled air. The respiratory system consists of nostrils, naso pharynx, pharynx, larynx, trachea and tracheo-bronchial tree. The tracheo-bronchial tree starts from trachea which is considered as generation 0 (G0). Trachea divides itself into two bronchi, left and right, which further individually bifurcate themselves dichotomously into bronchioles. There are total 23 generations in tree and the last stage is called alveolar region. This region is surrounded by blood capillaries. The respiratory sub-system from nostrils to 16th generation of the tree, termed as conductive airway, is responsible for cleaning, conditioning and humidifying the inhaled air. The remaining part of the tree, called as respiratory airway, facilitates gas exchange between air in alveoli and pulmonary blood in capillaries (Guyton and Hall (Guyton and E Hall, 2006).

The flow of air in conductive airways is dominated by convection process and diffusion process starts pre-dominating as the air moves distally down the tract. The equilibrium of convection and diffusion processes occur at G16-17. Hence the rate of ventilation and inspiration cycle plays key role in flowing the air distally down the tract (Keener and Sneyd, 2009). Depending on the condition of inhaled air, the respiratory organs have to work to filter, condition and humidify it properly. Thus the major challenge for the respiratory system is to finish its task before the inhaled air reaches at G17. If the non-conditioned or non-filtered air crosses G17, it interrupts the process of gas exchange by dehydrating or damaging tissues/cells in the alveolar region.

To prevent alveolar capillary bed interface from getting dehydrated, inspired air must be adjusted to body core temperature and full water saturation in a distributed and coupled fashion (Hanna and Scherer, 1986; McFadden, 1992) and the location where air reaches this condition is termed as iso-thermic saturation boundary (ISB). The conditioning of air is accomplished as the air stream flows through the respiratory tract to exchange heat and water vapor with the mucus membrane lining the airway surface (Pierce and Worsnop, 1999). If the air is warm, its capacity to hold water increases and it is humidified by evaporation process from the airway lining. The mucosa surfaces exchange heat through conduction and convection processes with the air

* Corresponding author.
E-mail addresses: bharat25soni@gmail.com (B. Soni), ameeyakumar@gmail.com (A.K. Nayak).

https://doi.org/10.1016/j.jtherbio.2019.07.026
Received 19 April 2019; Received in revised form 9 June 2019; Accepted 25 July 2019
Available online 30 July 2019

Nomenclature

subscripts

0	steady state
a	air
BT	body core temperature
b	blood
m	mucus
sat	saturated
t	tissue
w	water
A	Cross sectional area (cm^2)
C	Concentration of water (Kg/m^3)
c	Specific heat capacity ($J/Kg/K$)
D	Hydrolic diameter (cm)
H	Heaviside function
H_r	Relative humidity
h_c	Heat transfer coefficient between mucus and air ($W/m^2/K$)
h_{c1}	Heat transfer coefficient between tissue and mucus ($W/m^2/K$)
h_m	Metabolic heat generation rate (W)
I/E	Ratio of inspiration to expiration time.
k	Thermal conductivity ($W/m/K$)
L	Latent heat of vaporization (J/Kg)
l	Length of respiratory tract (cm)
m_c	Mass transfer coefficient (sec/m)
P	Perimeter (cm)
p	Pressure (KPa)
r	Radial direction in cylindrical coordinates
T	Temperature of air (K)
T_{b0}	Blood temperature at $z = 0$
t_b	Breathing time of one complete cycle
t	Time (sec)
U	Velocity of air (cm/sec)
$\dot{V}$	Air ventilation rate (L/min)
z	Axial direction in cylindrical coordinates

Greek symbols

α	Diffusivity of water in air (m^2/sec)
β	Non-dimensional number related to Re
γ	Non-dimensional number related to Re
δ	Position of mid-trachea
ρ	Air density Kg/m^3
ν	Kinematic viscosity m^2/sec
∇	Del operator

Non dimensional numbers

Nu	Nusselt number ($h_c D/k$)
Pr	Prandtl number ($\rho c\nu/k$)
Re	Reynolds number (UD/ν)
Sc	Schmidt number (ν/α)
Sh	Sherwood number ($m_c D/\alpha$)

during inhalation and use the latent heat of evaporation to conserve body heat and regulate temperature. The physics and physiology of the respiratory tract are such that the ability of the airways to recover heat and water is largely based on the size of the air stream-mucosal temperature gradients. Since the heat capacity of air is very low and hence warming is greatly facilitated by turbulent flows due to mixing effects provided by gas interaction with airway surfaces (Proetz, 1951). Also, during the tidal breathing at low ventilation rate, the convection process is responsible for air conditioning of laminar flow.

The major amount of gas exchange occurs at the alveolar membrane due to diffusion process. However, the significance of gas exchange extensively depends on: (I) solubility of gas with blood, (II) temperature dependence on solubility and (III) the degree of cooling experienced by the airway mucosa (Tsu et al., 1988). The last reason is relatively more important for interaction of heated air with airway walls. Again, the cooling performance is markedly depend on the inspired air condition, ventilation and the breathing pattern.

The wide and sudden variations in ambient inspiratory conditions challenge continuously varying thermal and fluid demands, mostly in the upper respiratory tract where most of the conditioning takes place (Hanna and Scherer, 1986; Xu et al., 2017). Inhalation of hot gases may burn the respiratory tract (Lv et al., 2006), while extreme cold air for long duration be a cause of cellular injury (Mortiz and Weisiger, 1945). However, the suitable temperature range of inhaled air depends on the state of the individual's airway and their tidal and minute volume (Shelly, 2001). Thus, there is an essential need to keep the track of heat exchange for varying inhalation temperatures.

Variations in ventilation rate affect the heat transfer efficiency. At low levels of ventilation, upper air passages play important role in air conditioning whereas role of tracheobronchial tree comes into the picture as the ventilation rises. For significantly high ventilation rate incompletely conditioned air penetrates deeply into intra-thoracic airways before it is brought into equilibrium with body core temperature (Ingenito et al., 1986; Wu et al., 2014) and the comparative analysis of the same is the primary motive of this article. Also, in such cases additional air conditioning must take place in the intra-thoracic airways in order to completely condition the inspired air to alveolar condition (McFadden, 1983).

The airway structure in the human upper airway is quite complicated as the range of the human breathing rate is widely varying from 0.5 to 5 L per breath. It may show the regimes of laminar, laminar-to-turbulent transition and turbulent air flow. With the gradual decrease in cross sectional area of the mouth-throat, naso-pharynx and pharynx-larynx, the velocity of the airflow increases rapidly and causes a transition from the laminar to the turbulence and in some area may even result in separation of boundary layer (Xu et al., 2017) because of convection dominance and this may require an accurate turbulence modeling. However, for tidal breathing the airflow can be assumed purely laminar for healthy lungs (Tsu et al., 1988) up to certain range of ventilation.

Although, *in vivo* measurements are more preferable but experiments related to the temperature with in nasal cavity or airway are limited due to complex anatomy. Temperature and humidity measurements are compact spatial and limited time resolution. To fill this gap, mathematical model is constructed which proves as a better tool in study of dynamic events. Several mathematical and computational models have been developed to study heat and water vapor concentration. Due to simplicity and less computational cost, one-dimensional (1D) and two-dimensional (2D) models are considered mostly (Hanna and Scherer, 1986; Tsu et al., 1988). The three dimensional (3D) models are although computationally more demanding but they provide more accurate temperature and velocity profile and hence used in this article. Some researchers have done 3D simulation work: for steady state (Xu et al., 2017) and for transient state (Lv et al., 2006, Wu et al., 2014) using computational fluid dynamics (CFD) approach but lacks mathematical approaches. Another problem which 1D or 2D models face are due to boundary conditions. In case of effective hot/cold air inspiration, the elements of air near to the wall goes in thermal exchange quite more rapidly than the elements at center of lumen. This makes 1D or 2D model less significant.

The problem with the transient 3D model for simulation is that, one needs to specify all the initial and boundary conditions for airway temperature at beginning itself but since they are dependent on the local air thermal dynamics and the thermal characteristics of adjacent compartments, the simulation results may not be that much accurate for this study. To get rid of that situation in simulation work, few researchers have simplified the airway geometry by considering it as regular (Lv et al., 2006), while few have done 1D simulation to get boundaries for 3D model (Wu et al., 2014) and the numerical algorithm is modified accordingly to deal with that problem.

Most of the previous studies dealt with heat, water vapor and soluble gas exchange in respiratory tract, analyzed the dynamics of airway and air temperature and air velocity profiles (Zhang and Kleinstreuer, 2003; Goodarzi-Ardakania et al., 2016; Xu et al., 2017) but very few have included the role of mucus - non perfused tissue layer (Lv et al., 2006; Wu et al., 2014) and capillary blood role (Hanna and Scherer, 1986; Tsu et al., 1988; Tawhai and Hunter, 2004). The another limitation with previous studies is related to the use of regular airway geometry which give tolerable results only for certain range of ventilation and temperatures (refer Fig. 10).

The above mentioned models have analyzed the impact of either the ventilation rates with fixed breathing pattern (Tawhai and Hunter, 2004; Goodarzi-Ardakania et al., 2016; Phuong et al., 2016) or varying breathing patterns with the fixed ventilation rate (Ingenito et al., 1990). The use of multi-compartmentalization approach is also been used in the past to study the dynamics of heat, water vapor and soluble gas (Tsu et al., 1988) but was limited to heat exchange by convection process only not by evaporation and conduction in radial direction.

In this article, a transient thermo-fluid model is proposed to study the heat exchange phenomena in human cast-replica respiratory tract during inspiration for tidal breathing. The model considers the effect of varying ventilation rates as well as breathing patterns to estimate the location of ISB. A multi-compartment control volume approach in cylindrical domain is considered to frame the model. This article also incorporates the thermal changes observed in mucus and non perfused tissue layers, with fixed thickness, which plays key role in the heat exchange during inspiration in different environments.

2. Mathematical model

The entire airway wall tissues contain a rich supply of blood vessels, lymph vessels and nerves. Numerous mucus glands are embedded in the tissues. Ciliated epithelial cells line the airway surface and continually move the mucus gel (also known as airway surface liquid (ASL) and have gel like structure), secreted by the mucus glands, towards the pharynx. The main role of mucus layer is to make air free from debris and foreign particles and to condition the inhaled air.

The thickness of the mucus layer varies as liquid evaporates from or condenses to mucus membrane. On reduction of mucus thickness to minimum value, non-perfused tissue trigger the secretion of ASL in mucus to prevent dehydration. The water evaporation control the volume of mucus layer (Karamaoun et al., 2018). Capillaries filter the liquid to maintain the hydration of non-perfused tissue layer. Healthy mucus gel have very low viscosity and elasticity and hence can be easily transported in ciliary actions (Fahy and Dickey, 2010) and thus the assumption of constant thickness can be considered accurate in healthy cast replica models. Arrow marks in Fig. 1 shows that the liquid loss from the mucus by evaporation is replenished by liquid secretion from tissue and filtration from capillaries. The gel undergoes spontaneous swelling and the hydration of gel is controlled by membrane transport of ions and water in *Gibbs-Donnan type equilibrium process* (Girod et al., 1992).

Mucus is a poly-ionic gel which contains two types of water, bound water in the gel matrix and free water. Initially free water evaporates from the mucus gel. However, a much lower pressure of the bound water makes it resistant to evaporation and further drying of the mucosal surface may stimulate secretion of more free water from the underlying tissue (Randell and Boucher, 2006). Diffusion of water through the mucosa is assumed to be governed by *Fick's law*.

To frame the mathematical model to study the heat exchange in

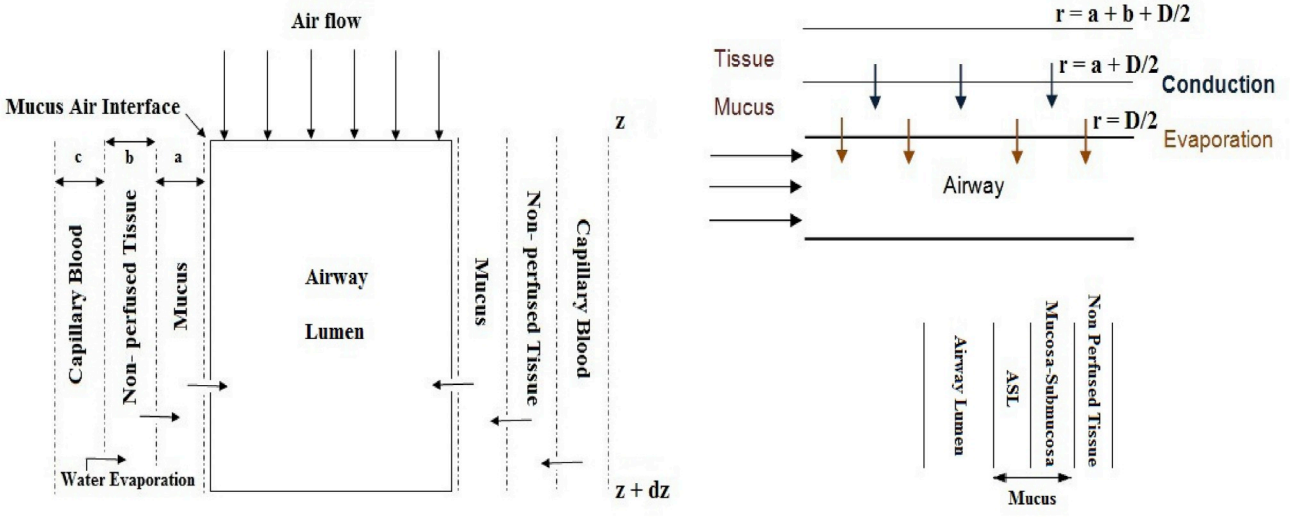

Fig. 1. Bird's Eye view of air flow in infinitesimal finite volume domain of human respiratory tract.

$$\frac{\partial \vec{U}}{\partial t} + (\vec{U}.\nabla)\vec{U} = -\frac{1}{\rho}\nabla p + \nu\nabla^2\vec{U}, \tag{1}$$

$$\frac{\partial T}{\partial t} + (\vec{U}.\nabla)T = \frac{k}{\rho c_p}\nabla^2 T, \tag{2}$$

$$\frac{\partial T_a}{\partial t} + U(t;z)\frac{\partial T_a}{\partial z} = \frac{P(z)}{\rho_a c_a A(z)}\left[h_c(T - T_a) + L\frac{(p_{sat,a} - H_r p_{sat,t})}{m_c}\right]. \tag{3}$$

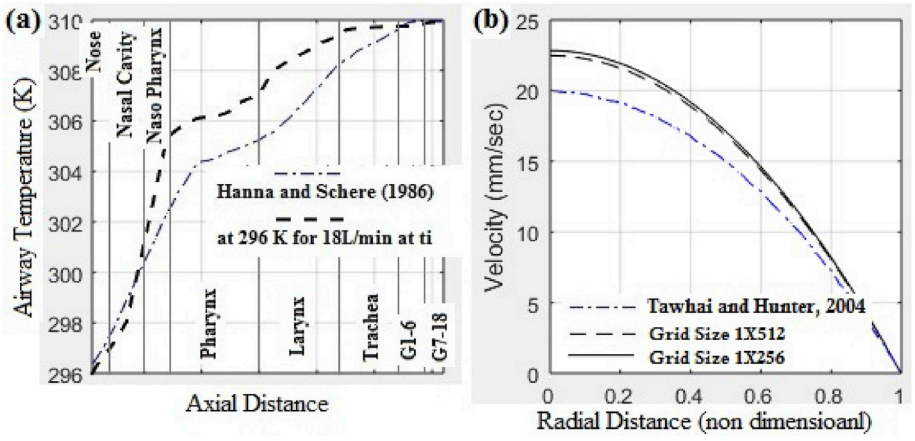

Fig. 2. Result validation (a) for Tainsp = 296 K and tb = 5 sec at the end of inspiration cycle with experimental results. (b) for radial velocity when $\gamma = 2$ at Trachea.

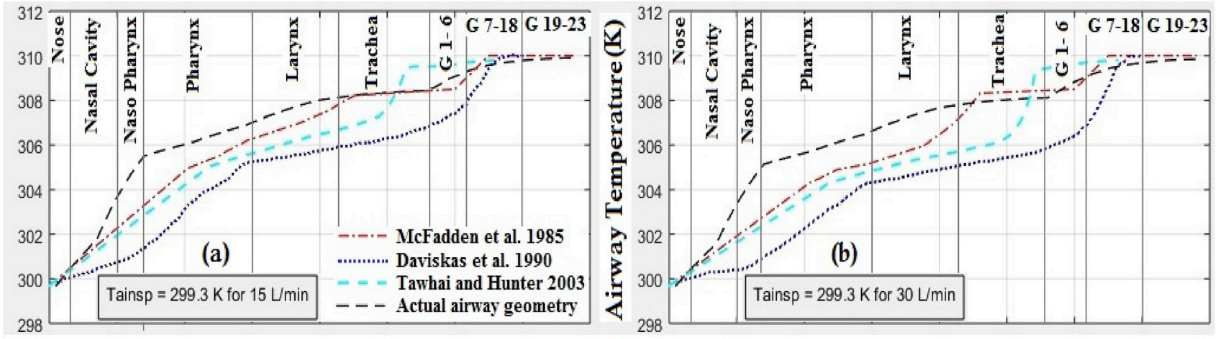

Fig. 3. Validation of results for $T_{ainsp} = 299.3K$ for (a) 15 L/min and (b) 30 L/min ventilation rate.

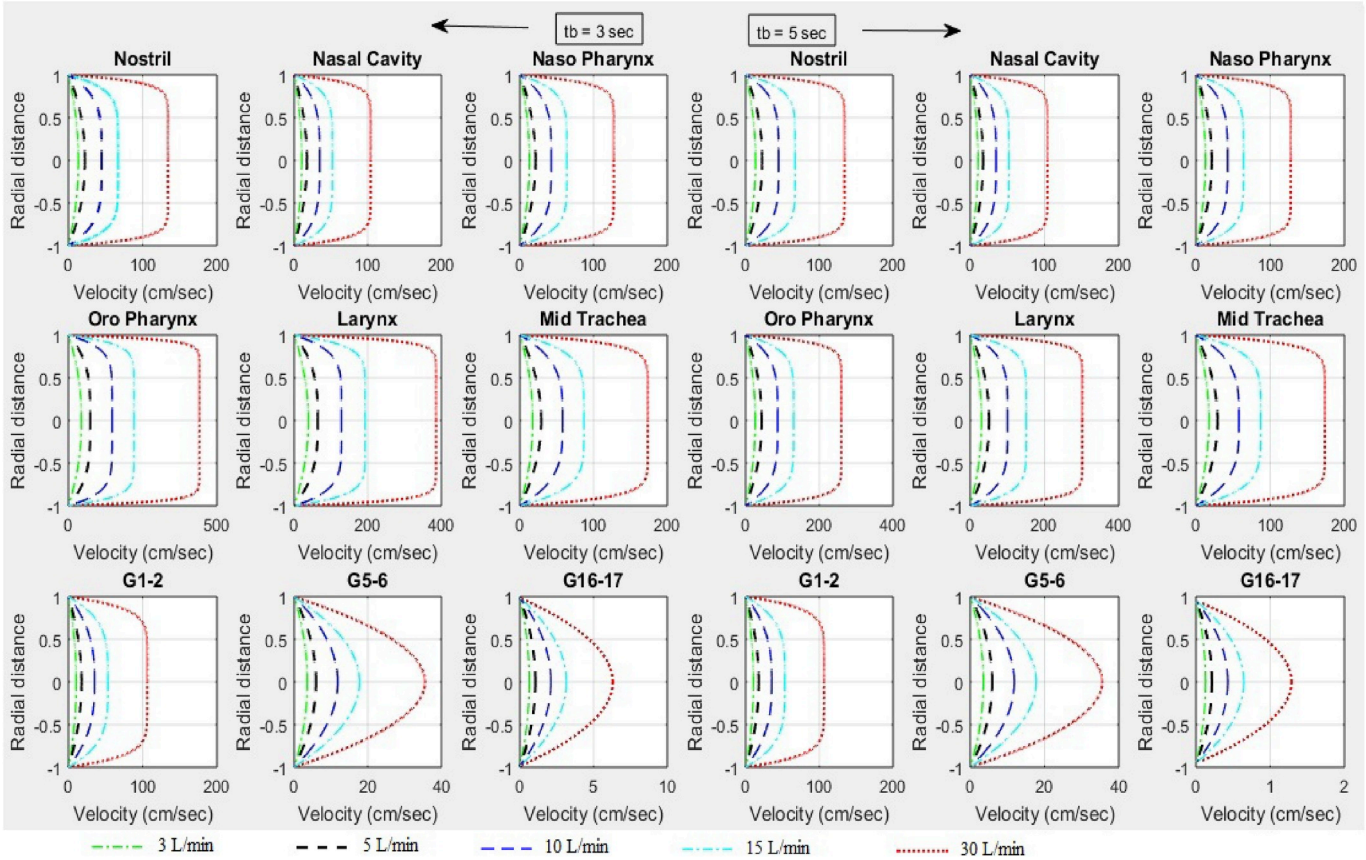

Fig. 4. Air velocity in radial direction for breathing time $t_b = 3$ sec with I/E ratio 2:1 and $t_b = 5$ sec with I/E ratio 3:2 for $\dot{V} = 3$, 5, 10, 15 and 30 L/min.

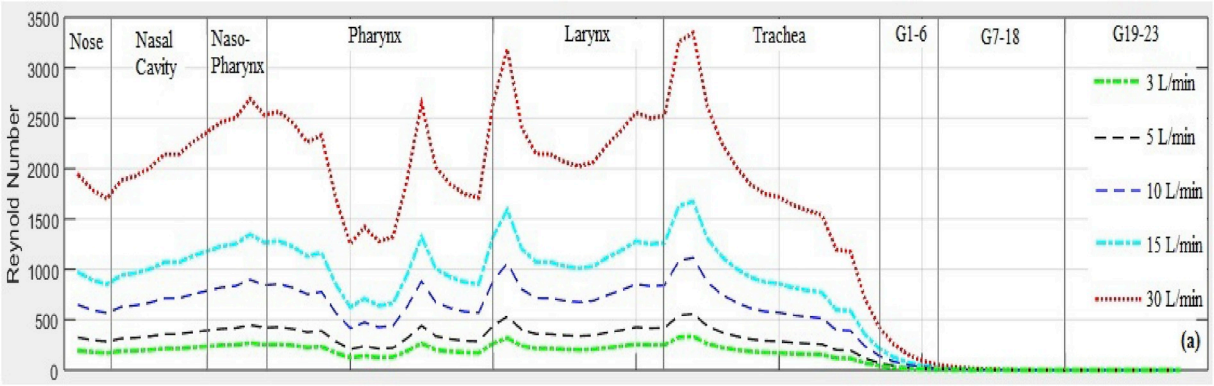

Fig. 5. Variation of Reynolds number with distance.

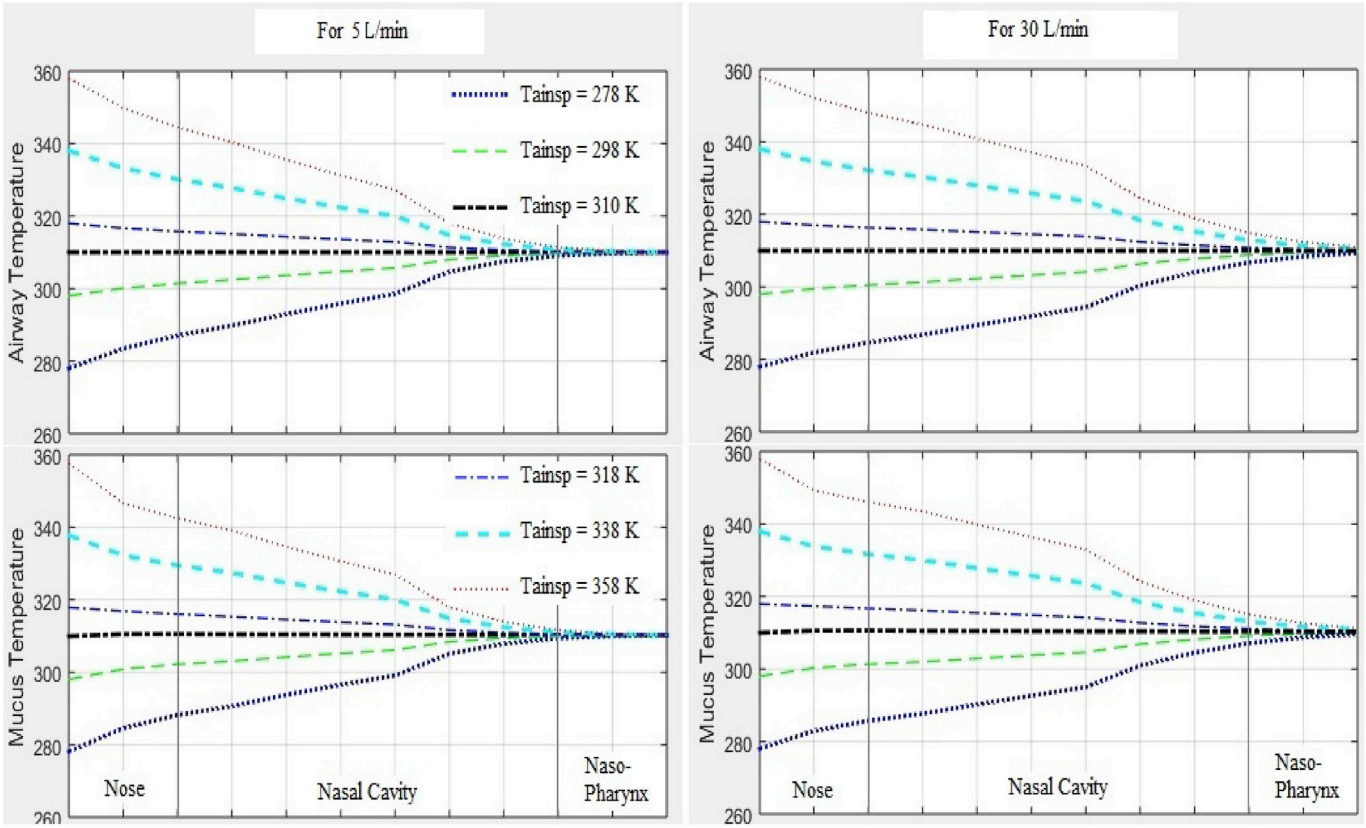

Fig. 6. Settling of airway temperature at saturation at the time of the air heat enters into the nose ($t = 0^+$).

human airways, a multi-compartment cylindrical control volume (CCV) approach is used. The CCV of airway is radially sectioned into three regions: the airway lumen, thin mucus layer of width a and an underlying layer of non-perfused tissue of width b. A capillary bed lies beyond the non perfused tissue layer with blood temperature T_b. Bird's eye view of this schematic is shown in Fig. 1.

The control volume of a compartment offers many advantages to analyze the heat dynamics; (I) It does not require the exact complete knowledge of airway dimension and hence not require the information of exact velocity profile, (II) It can handle the complex domain easily and (III) Using volume average concept, heat, mass and momentum transfer rates can be evaluated and by law of conservation at boundaries, they can be further used as boundary conditions for adjacent compartments. The refinement of the size of compartments allows fine tuning in physical observations but the same requires more morphological data sets. Thus, clinically it can help in the study of dynamics by feeding the dimensions of airway. Also, in many of the disease cases, there are significant changes at only few locations and which can be easily incorporated and reduce the computational costs.

The airway walls are considered to be rigid, diathermic and impermeable for incompressible air flow with constant density and no slip boundary conditions. The air tube is taken axisymmetric with respect to the direction of the airflow. The flow of air is taken in both r and z directions but both are assumed to be independent to each other. Similarly, surrounded layers of mucus, non perfused tissue and capillary bed are studied in both radial and axial directions. During inhalation, $z = 0$ is taken at nostril and $z = l$ is at alveolar region.

Eq. (1) is Navier Stokes equation in cylindrical coordinate system for flow of air in axisymmetric airway tube. The radial component of velocity is treated independent to axial direction and vice versa. Both radial and axial direction velocity components are function of breathing cycle and hence depend on time. In these model equations, $0 \leq t \leq t_b$

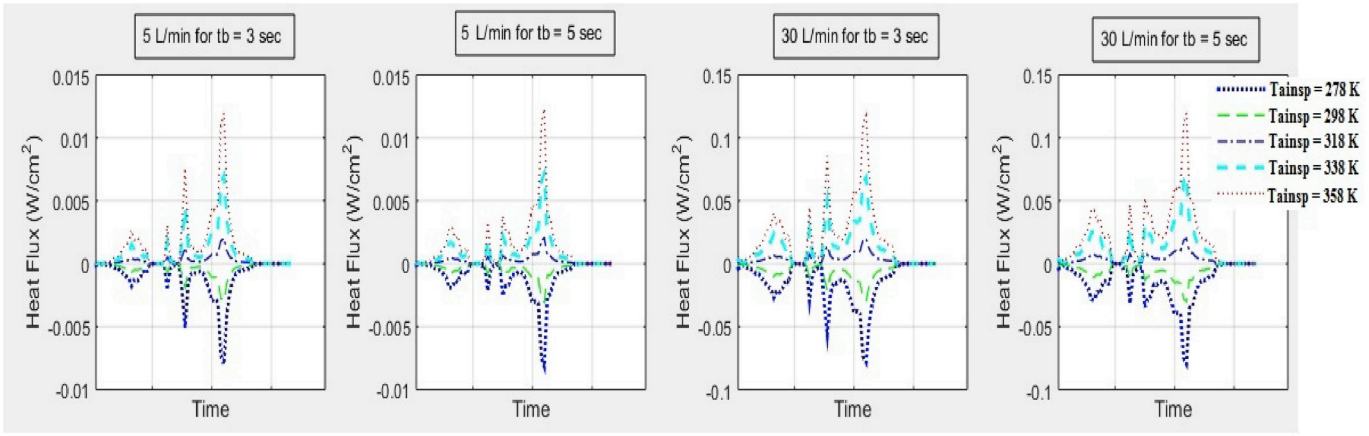

Fig. 7. Variation of heat flux with respect to time at trachea.

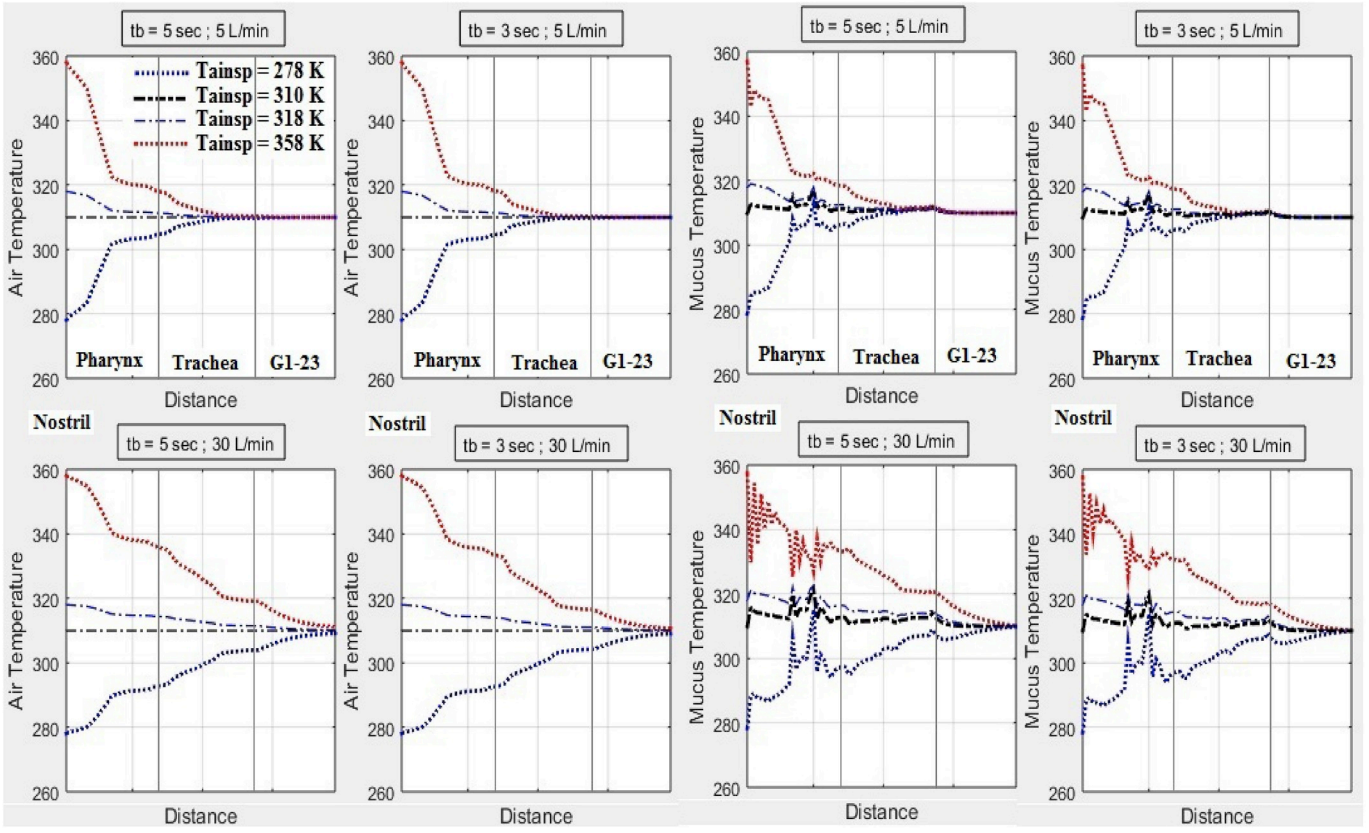

Fig. 8. Settling zone (ISB) of inspired air for various temperatures at end of inspiration ($t = t_I$) - actual geometry.

where t_b is one complete cycle of tidal breathing. It has already been proved biologically that the total pressure drop is very negligible for tidal breathing (Olson et al., 1970) so pressure gradient can be neglected. Eq. (2) is energy balance equation for airway temperature T in control volume given in Fig. 1 which considers no heat loss from respiratory tract. The concentration of water vapor in air is assumed constant. The energy balance equation for air temperature due to convection and evaporation processes with mucus surface is given by Eq. (3). The air temperature gradients in axial direction due to conduction are very small as compared to that of in radial direction and hence are neglected. The radial and axial components of velocity are varying only in their respective directions. Since airway walls are considered rigid, the geometry of wall is not get altered during flow.

The qualitative agreement among biologist and scientists suggest that the local blood temperature in nasal or oral compartment can be assumed $305K$ or $307K$ respectively and varies linearly up to mid-trachea and level off at body core temperature for all distal compartments (Hanna and Scherer, 1986; Tsu et al., 1988) which is given by Eq. (4).

$$T_b = T_{b0} + [H(z) - H(z-\delta)]\left(\frac{T_{BT} - T_{b0}}{\delta}\right)z. \tag{4}$$

2.1. Initial and boundary conditions

The initial condition for model is given by Eq. (5).

$$T = T_a = T_m = T_0, \quad \text{at } t = 0 \tag{5}$$

where T_0 is steady state temperature which is in synchronization with initial air temperature $T_0 = T_{insp}$ at $z = 0$. For solving the set of model equations (1)–(3), the airway heat flux is assumed to be zero at

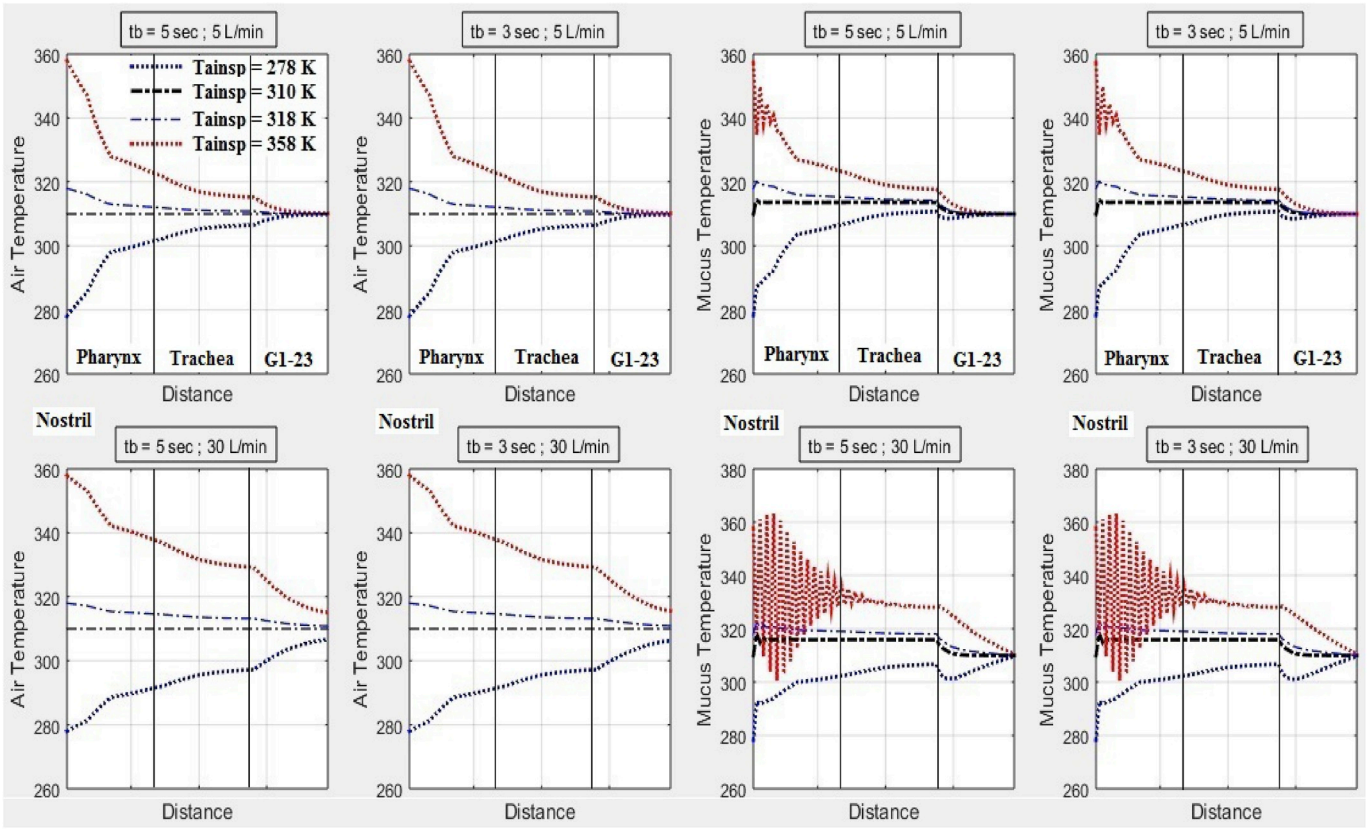

Fig. 9. Settling zone (ISB) of inspired air for various temperatures at end of inspiration ($t = t_I$) - regular geometry.

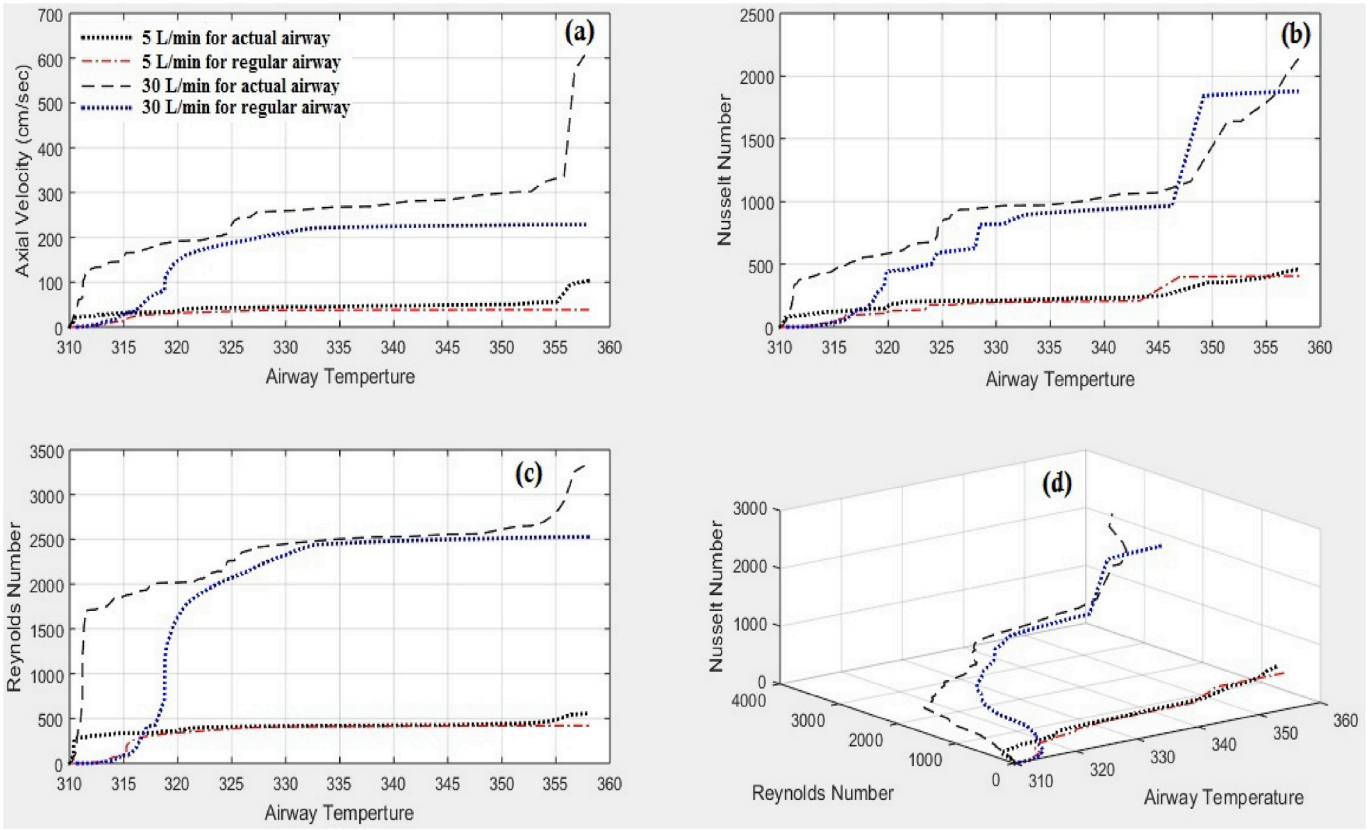

Fig. 10. Comparison of regular airway geometry with actual geometry at $Tainsp = 358K$ for $tb = 5sec$.

boundaries of blood-tissue, tissue-mucosa and mucosa-wall ($r = a + b + \frac{D}{2}$, $r = a + \frac{D}{2}$ and $r = \frac{D}{2}$ respectively) which is given as:

$$\frac{\partial T}{\partial r} = 0. \tag{6}$$

The axial boundary conditions for air temperature T_a for inspiration ($0 \le t \le t_I^-$) and expiration ($t_I^+ \le t \le t_b = t_I + t_E$)phases are given as:

$$T_a(z = 0) = T_{ainsp}, \quad \frac{\partial T_a}{\partial z}(z = l) = 0; \quad 0 \le t \le t_I^-, \tag{7}$$

$$\frac{\partial T_a}{\partial z}(z = l) = 0, \quad T_a(z = 0) = T_{BT}; \quad t_I^+ \le t \le t_b. \tag{8}$$

The inlet (outlet) convective boundary condition for inspiration (expiration) phase at $z = 0$ for airway temperature T is imposed by using equilibrium condition of heat flux, given in Eq. (9).

$$k\frac{\partial T}{\partial z} = h_{c1}(T - T_{ainsp}); \quad \text{at } z = 0. \tag{9}$$

2.2. Temperature estimation at mucus layer

At boundary $r = \frac{D}{2}$, the heat is exchanged between air and mucus membrane by convection and evaporation and obtains equilibrium with blood temperature via layer of non-perfused tissue by conduction, which is given by Eq. (10). The temporal changes in mucus membrane temperature are very small (Tsai et al., 1990) and hence can be ignored to reduce the complexity of model.

$$k_t\left(\frac{T_l - T_m}{a} + \frac{T_b - T_l}{b}\right) = h_c(T_m - T_a) + \frac{L(C_{w,m} - C_{w,a})}{m_c}. \tag{10}$$

The empirical relation between water vapor concentration at mucus interface $C_{w,m}$ and mucus temperature T_m for 100% relative humidity (H_r) is given by Eq. (11).

$$C_{w,m} = \frac{2.166 \times 10^{-3}}{T_m} e^{\left(\lambda_1 + \frac{\lambda_2}{T_m} + \lambda_3 \ln(T_m) + \lambda_4 T_m^2\right)}, \tag{11}$$

where $\lambda_1 = 73.649$, $\lambda_2 = -7258.2$, $\lambda_3 = -7.3037$ and $\lambda_4 = 4.165 \times 10^{-6}$ (Tawhai and Hunter, 2004; Wu et al. 2014).

2.3. Temperature and velocity estimation in radial direction

The profile of air temperature T_a and air velocity U in radial direction are assumed to follow power law as described in Eq.(12-13). The advantage to consider this power law model is that it is integrable in domain of problem.

$$T_a(r) = T_{aR} + (T_{a0} - T_{aR})\left[1 - \left(\frac{2r}{D}\right)^{\beta}\right], \tag{12}$$

$$U(r) = U_0\left[1 - \left(\frac{2r}{D}\right)^{\gamma}\right], \tag{13}$$

where $T_{a0} = T_a(t; z, 0)$ and $U_0 = U(t, z, 0)$ are temperature and velocity respectively obtained at center of airway tube while $T_{aR} = T_a(t; z, D/2)$ and $U_0 = U(t, z, D/2)$ are corresponding values obtained at fluid-wall interface for all $0 \le r \le \frac{D}{2}$. The value of β $(=\gamma)$ is taken as 2 for $Re < 300$ while taken as $\frac{Re}{150}$ for $Re \ge 300$. (Saidel et al., 1983; Tawhai and Hunter, 2004).

2.4. Local morphological data set

The geometry of the airway conduit is neither perfectly circular nor regular hence be the cause of non-uniform air conditioning (Hanna and Scherer, 1986). In past, the air conditioning process is studied analytically only for regular geometry airway tube (Tawhai and Hunter, 2004; Lv et al., 2006). However, for low ventilation rate regular geometry can produce adequate results but during mechanical ventilation or during exercise or for high ventilation case which occurs when demand of oxygen increase, the regular geometry does not give satisfactory results and hence need the actual geometry of airway. Since it's very difficult to measure all the geometrical data points and also these values vary with age, sex and ethnicity, cast replica model can help in generalizing the theory.

To avoid topological error in the theoretical mathematical model, there is a need to know the regional values of $P(z)$ and $A(z)$. The local information has been obtained from available cast replica airway model where perimeter and cross sectional area values are estimated starting from nasal cavity to trachea (Cheng et al., 1997). The variations in coronal and sagittal planes are not considered and this make the geometry axisymmetric in nature. The hydraulic diameter $D(z)$ is evaluated based on these geometric information. For estimating the diameters of tracheo-bronchial tree generations, classical Murray's law for minimization of flow resistance is applied which suggest that ratio of parent to daughter tube diameters and lengths are $2^{1/3}$ at each generation. The structure of tracheo-bronchial tree is considered to be symmetric.

2.5. Local heat and mass transfer

Physiologically, heat transfer coefficient (HTC) values play key role in studying the transfer of thermal power for varying breathing conditions to condition the air (Phuong et al., 2016) and further play key role in determining the gas exchange (Goodarzi-Ardakania et al., 2016). By using *Chilton - Colburn analogy*, the local heat and mass transfer coefficients are correlated which assumes equal heat and mass transfer in movement of fluid with certain range of *Pr* and *Re*. Several authors represented mathematical relation in terms of *Nu* and *Sh* to relate heat and mass transfer by either experimental methods (Hanna and Scherer, 1986) or simulation (Zhang and Kleinstreuer, 2003). The heat transfer coefficient h_c and mass transfer coefficient m_c between mucus surface and flowing air are evaluated from physiological data by naphthalene sublimation experiment (Hanna and Scherer, 1986). For inspiration phase, the relations are given as:

$$Sh = c_1 Re^{0.856} Sc^{1/3}; \quad \text{for } 0 \le t \le t_I^-, \tag{14}$$

$$Nu = c_1 Re^{0.856} Pr^{1/3}; \quad \text{for } 0 \le t \le t_I^-. \tag{15}$$

where c_1 is local constant but vary with compartments.

3. Numerical method

The above mathematical model is solved numerically using higher order finite difference approximation on each compartment to find the local solution. Later, using the continuity of mass, momentum and heat at common surfaces of local compartments, the global perspective is presented as result.

The axial velocity components at inlet are derived from ratio of given ventilation rate and nostril cross sectional area. Numerically, it was solved for one direction keeping another constant till the results are accurate up to the order of 6. Also, after finding the axial and radial component of the same compartment, the effect of heat is analyzed in the next compartments for initial thermal boundary conditions of airway and airway wall. Since the blood temperature is assumed to obey a simple relation, the tissue layer temperature can be derived by average of mucus layer and blood temperature. This is an iterative process and stops till the steadiness arrives for the same. All the equations were solved for fixed time at global level and then transient analysis is done to find the temporal changes.

3.1. Multi-compartmentalization

The morphological datum of cast replica model from nostril to trachea end are available at each 30mm distance. Each such zone of length 30mm is considered as single compartment. The length and diameter of trachea are taken as 10cm and 1.8cm respectively. The G1 of tracheobronchial tree is considered a single compartment and for G2-G23 each compartment consist two generation stages. In sum, the complete respiratory tract is sectioned into 67 compartments.

4. Model validation

Since a cast replica theoretical model is analyzed therefore the results differ from the past studies because of the variations in airway geometry and breathing conditions. Many of the past results dealt with regular geometry (perfectly circular cross section throughout the tube length). A few researchers have employed geometry data points obtained from either cast replica model or CT scan. The results are validated not for exact distance from inlet but for the equivalent physical location (compartment) because of the significant difference in subject's airway geometry.

The flow of air mass depends on the rate of ventilation and inspiration cycle whereas the flow of air heat depends on the inspiratory temperature. As discussed in the introduction section, the most of the heat exchange phenomena occurs in upper respiratory tract which is the conductive zone. Hence ideally, the inhaled air should get saturated before generation 16–17.

To validate our model, the length of tract is properly transferred to match the tract with previous studies. Fig. 2–3 show the comparison of results for various cases. The test for grid independency is executed by changing the grid size from 1×256 to 1×512 and it is found that the size 1×512 is optimal.

5. Results

In order to capture the convective heat exchange dynamics during one complete breathing cycle, the study of air velocity behavior is important which varies with breathing frequency, rate of air ventilation and airway diameter. Two different sinusoidal breathing patterns are considered in this article, one with $t_b = 3$ s with I/E ratio 2:1 and another is $t_b = 5$ s with I/E ratio 3:2.

Fig. 4 shows the radial distribution of air velocity inside airway for both $t_b = 3$ and 5 sec during inspiration which follows Eq. (13). In all the sub-figures, the nature of velocity is influenced by γ which relates Reynold's number (Re). The method of γ calculations has already been discussed in section 2.3.

As the rate of ventilation increases, it makes air to flow with different radial characteristics varying from order 2 (Poiseuille) and is higher in intra-thoracic compartments for tidal breathing. Further, a markable observation is also made with respect to the inspiration to expiration time ratio. Since, we have considered the case of tidal breathing so flow remains in laminar regime at all compartments for considered ventilation values 3, 5, 10 and 15 L/min as shown in Fig. 5. The air flow behaves turbulent even for tidal breathing in case of ventilation rate 30 L/min. If inspiration time is high then this turbulence can be controlled before the G16-17 but not at trachea.

For $t_b = 5$ sec, the flow achieves the second order Poiseuille flow characteristics at the end of mid trachea while for $t_b = 3$ sec, the same is achieved at G 1–2 for air ventilation 10 and 15 L/min. For low ventilation value, the flow characteristics are almost similar for both $t_b = 3$ and 5 sec while at higher ventilation rates, the flow nature differs by significant amount. Thus breathing at slight faster rate can mix the heat with distal air because of turbulent flow and may lead to damage in tissues if it penetrates deep into tract.

As the subject starts breathing i.e. before the mass of inspired air crosses the cross section of the nostril, the heat of air bring impact on tissues at inlet. Because of thermal conductivity of tissues, the heat penetrates inside the tract till it made to settle at saturation level by mucus layer. The distance of this penetration depends on the rate of ventilation and inspired air temperature. As shown in Fig. 6, for temperature values 298 K, 310 K and 318 K, the nasal-cavity tissues have to perform negligible amount of work to bring the state of saturation but if the temperature is either very cold (278 K) or very hot (338 K and 358 K), it travels complete nasal cavity to achieve the saturation. Further, if ventilation rate is high then the effect of thermal work can be observed in the region of naso pharynx as well. These results do not much depend on the breathing cycle because they are observed when the air is at inlet and subject has just initiated the breathe.

Once the subject finish her/his inspiration cycle, the exchange of convective heat transfer still remain progressive, simultaneous with gas exchange process at alveolar region. The mucus layer, non perfused tissue layer and capillary blood are in the state of working to bring all the tissues at the saturation level. In case of healthy subject with tidal breathing, the same is achieved during the process of gas exchange at alveolar region itself but for subject with severe obstructive disease and breathing forcefully, the same is not guaranteed.

The corresponding time variations in heat flux values for various inhalation temperatures for both breathing patterns and ventilation rates 5 and 30 L/min at mid trachea are shown in Fig. 7. For same breathing cycle, as the rate of ventilation increases, the overall rate of heat exchange increases while as the inspiration time increases, the overall rate decreases. It can also be observed that when the inhaled air reaches at trachea, the downstream adjacent compartment have more steeper change in heat flux than the rest compartments.

Fig. 8 shows the thermal settling zone of inspired air and mucus layer for various temperatures (278 K, 310 K, 318 K and 358 K) for both breathing patterns ($t_b = 3$, 5 sec) at 5 L/min and 30 L/min. It can be observed that for low ventilation rate (5 L/min), the changes in ISB locations for different observed inhalation temperatures are significant. This effect gets quite significant as the rate of ventilation increases. For mild temperatures, the effect of breathing cycle is present but for extreme temperature conditions (either too cold or hot), the ISB achieved in almost same compartments in case of both the breathing patterns.

The results for same set of ventilation rate and inhalation temperature are carried for the case of regular airway geometry considering the diameter of tract from nostril to trachea same as that of trachea (Fig. 9). It is observed that for high ventilation (30 L/min) the results differ significantly with actual geometry. The mucus temperature shows oscillatory nature in pharynx which is nothing but the thermal noise and hence based on this observation, it can be interpreted that regular geometry is not correct for high ventilation case.

To differentiate the effect of actual geometry, the entire cast replica model is solved for two cases: I. cast replica model with actual diameter and perimeter value and II. model with same diameter and perimeter of tube from nostril to trachea. In both the cases, the Murray's law is considered to find the diameters of tracheo-bronchial tree. For both the models the results are plotted with respect to airway geometry, the variations of axial velocity, Nusselt number and Reynolds number with airway temperature in Fig. 10 for the case of $Tainsp = 358K$, $t_b = 5sec$ and $\dot{V} = 5{,}30$ L/min. It can be observed clearly that for the case of tidal breathing low ventilation, there is no much significant effect of airway geometry but for high ventilation the same give high impact. The difference between maximum Reynolds and Nusselt number observed confirms the importance of regular geometry.

6. Discussion

The respiratory system is the body's first line defense against the unconditioned air and debris inside the air. An investigation about the airflow provides valuable information about movement of heat and pollutants. The healthy respiratory system is designed in such a way that it condition the most part of air in upper respiratory tract and

blocks the pollutants. This study comprise of only heat exchange. It is the velocity of air only which help heat to move deep inside the tract during the process of conditioning, for convection dominated region.

The air velocity inside tract is influenced by ventilation rates. The higher the local ventilation, the more air needs to be conditioned by respiratory system within given amount of time. This amount of time is provided by inspiration cycle. The more the time spends for inspiration, the more the chance for air to be fully conditioned on or before G16-17.

The distribution of heat throughout the tract for given inspired temperature, ventilation rate and breathing time is very much sensitive to mathematical model. As already discussed, 1D model is unable to characterize the heat transfer in radial direction while 2D model does not provide accurate information at wall boundary. The problem of wall boundary still persists with 3D simulation work in many cases. To avoid such things, a temporal axisymmetric mathematical model is solved numerically and the local compartment's boundary conditions are obtained from downstream adjacent compartment. Thus this provides the continuity of heat, mass and momentum at compartment interface and thus helped in solving the model equations.

The local dynamic gradients between inspired air and mucus layer are very much dependent on the inspired conditions. At the beginning of the inspiration cycle, the mucosal condition are not known and hence to get these boundary conditions, the code has implemented on each compartment and the axial propagation distance has been measured (Fig. 8) and the results obtained at boundary are taken as new boundary conditions. Since the size of compartment is fine enough for accuracy, so the error in boundary values can be neglected.

Another parameter which influence the temperature distribution is the airway geometry. Because of highly irregular geometry, the process of air conditioning in respiratory tract is naturally dominated by convection-diffusion processes. Due to presence of these irregularities only, the flow is able to show the various regimes like laminar, laminar to turbulence transition and turbulence (Fig. 5). Several past studies captured the temperature distribution in imaginary regular airway geometry for ease of analysis. But this is inaccurate from both the aspect of physics and physiology. The assumption of regular geometry up to trachea end are not able to show the changes in flow characteristics and hence the proper air element mixing with mucosal layer and ASL for heat exchange can not be studied (Fig. 10).

The primary focus of this study was to check the effect of ventilation on temperature distribution and on ISB (Figs. 8 and 9). The significant variations were observed on ISB for same inhalation temperature with varying rate of ventilations. The ISB location shows remarkable changes if the airway geometry is considered regular. Another observation was made regarding breathing cycle. For the slow breathing, the inhaled air gets sufficient time to condition itself while at faster breathing rates, the location of ISB moved more distal down. This study was limited for the tidal nasal breathing only.

The location of ISB may also get affected by nasal or oral breathing. Under normal circumstances, the nasal breathing is quite more effective than the oral breathing in conditioning the inspired air and further in minimizing the heat and water vapor losses from the tract. Although the numerical investigation for the oral breathing case has not been executed in this article but biologically during mouth breathing, which is the case arise in exercise or hyperventilation, the heat and water vapor loss occurs abnormally.

Although during the expiration heat exchange is also in progress but this is of very negligible amount. As discussed earlier, the water is given back to the mucus layer. Since the role of water vapor molecules has not been studied explicitly in this article and hence this work only revolve around the heat exchange for varying inspiration cycles and ventilation rates during inhalation. The amount of relative humidity also be the cause in heat exchange especially in case of breathing during exercise.

The study of the more accurate or exact heat and water vapor exchange in human respiratory tract is a very complicated task. This includes the role of turbulence, separated flow at boundary and viscoelastic airway wall along with the knowledge of exact complete morphological parameters. Further the changes in chemical compositions at ASL layer, which also bring changes in its thickness, in the case of continuous breathing in ill-conditioned environment put a remarkable impact on thermal dynamics. This may further evoke the function of asthma because of improper heat exchanges. The role of perfused pulmonary blood also effect the heat and water vapor gradients which is quite related to the process of gas exchange. Also the blood flow in mucus and tissue layer play important role in the heat exchange but due to unavailability of exact local blood dynamics in cast replica model, we have considered theoretical values of blood temperature in capillary bed in healthy adult. The anatomical study of all such things are available up to some extent but the mathematical model for all these things is still not framed. This task will be tried to achieve the same in future part of this work.

7. Conclusion

In order to capture the thermal dynamics of healthy human respiratory tract during inspiration for tidal breathing, a multi compartment 3D theoretical model was established and the same was applied to study the patterns in the air and mucus-non perfused tissue layer. Effects of ventilation rate along with inspiration time are captured and concluded numerically that as the inspiration time decreases and/or ventilation rate increases, the chances of thermal injury of tissues increase. Since, the model is theoretical, the exact location of ISB can not be evaluated but can be predicted with respect to the compartment, which gave motive to apply the approach of multi-compartmentalization.

Acknowledgement

One of the Author Dr. A. K. Nayak kindly acknowledges the financial supportby the Alexander Von Humboldt fondation.

References

Cheng, K.H., Cheng, Y.S., Yeh, H.C., Swift, D.L., 1997. Measurements of airway dimensions and calculation of mass transfer characteristics of the human oral passage. J. Biomech. Eng. 119, 476–482.
Fahy, J.V., Dickey, B.F., 2010. Airway mucus function and dysfunction. N. Engl. J. Med. 363 (23), 2233–2247.
Girod, S., Zahm, J.M., Plotkowski, C., Beck, G., Puchelle, E., 1992. Role of the physicochemical properties of mucus in the protection of the respiratory epithelium. Eur. Respir. J. 5, 477–487.
Goodarzi-Ardakania, V., Taeibi-Rahnia, M., Salimia, M.R., Ahmadib, G., 2016. Computational simulation of temperature and velocity distribution in human upper respiratory airway during inhalation of hot air. Respir. Physiol. Neurobiol. 223, 49–58.
Guyton, A.C., E Hall, J., 2006. Medical Physiology, eleventh ed. Elsevier Saunders.
Hanna, L.M., Scherer, P.W., 1986. A theoretical model of localized heat and water vapor transport in the human respiratory tract. J. Biomed. Eng. 108, 19–27.
Ingenito, E.P., Pichurko, B.M., Lafleur, J., Drazen, J.M., Ingram Jr., R.H., Solway, J., 1990. Breathing pattern affects respiratory heat loss but not bronchoconstrictor response in asthma. Lung 168, 23–34.
Ingenito, E.P., Solway, J., McFadden Jr., E.R., Pichurko, B.M., Cravalho, E.G., Drazen, J.M., 1986. Finite difference analysis of respiratory heat transfer. J. Appl. Physiol. 61 (6), 2252–2259.
Karamaoun, C., Sobac, B., Mauroy, B., Muylem, A.V., Haut, B., 2018. New insights into the mechanisms controlling the bronchial mucus balance. PLoS One 13 (6).
Keener, J., Sneyd, J., 2009. Mathematical Physiology II : System Physiology, second ed. Springer.
Lv, Y.G., Liu, J., Zhang, J., 2006. Theoretical evaluation of burns to the human respiratory tract due to inhalation of hot gas in the early stage of fires. Burns 32, 436–446.
McFadden Jr., E.R., 1992. Heat and water exchange in human airways. Am. Rev. Respir. Dis. 146 S8-sS0.
McFadden Jr., E.R., 1983. Respiratory heat and water exchange: physiological and clinical implications. J. Appl. Physiol. 54, 331–336.
Mortiz, A.R., Weisiger, J.R., 1945. Effects of cold air on the air passages and lungs. Arch. Intern. Med. 75 (4), 233–240.
Olson, D.E., Dart, G.A., Filley, G.F., 1970. Pressure drop and fluid flow regime of air inspired into the human lung. J. Appl. Physiol. 28 (4), 482–494.
Phuong, N.L., Yamashita, M., Yoo, S.J., Ito, K., 2016. Prediction of convective heat transfer coefficient of human upper and lower airway surfaces in steady and unsteady

breathing conditions. Build. Environ. 100, 172–185.
Pierce, R.J., Worsnop, C.J., 1999. Upper airway function and dysfunction in respiration. Clin. Exp. Pharmacol. Physiol. 26, 1–10.
Proetz, A.W., 1951. Air currents in the upper respiratory tract and their clinical importance. Ann. Otol. Rhinol. Laryngol. 60 (2), 439–467.
Randell, S.H., Boucher, R.C., 2006. Effective mucus clearance is essential for respiratory health. Am. J. Respir. Cell Mol. Biol. 35, 20–28.
Saidel, G.M., Kruse, K.L., Primiano Jr., F.P., 1983. Model simulation of heat and water transport dynamics in an airway. ASME J. Bio-Mech. Eng. 105, 188–193.
Shelly, M.P., 2001. Editorial: the upper airway - the forgotten organ. Crit. Care 5 (1), 1–2.
Tawhai, M.H., Hunter, P.J., 2004. Modeling water vapor and heat transfer in the normal and the intubated airways. Ann. Biomed. Eng. 32, 609–622.
Tsai, C.L., Saidel, G.M., McFadden Jr., E.R., Fouke, J.M., 1990. Radial heat and water transport across the airway wall. J. Appl. Physiol. 69 (1), 222–231.
Tsu, M.E., Babb, A.L., Ralph, D.D., Hlastla, M.P., 1988. Dynamics of heat, water and soluble gas exchange in the human airways: 1. A model study. Ann. Biomed. Eng. 16, 547–571.
Wu, D., Tawhai, M.H., Hoffman, E.A., Lin, C.L., 2014. A numerical study of heat and water vapor transfer in MDCT-based human airway models. Ann. Biomed. Eng. 40 (10), 2117–2131.
Xu, X.Y., Ni, S.J., Fu, M., Zheng, X., Luo, N., Weng, W.G., 2017. Numerical investigation of airflow, heat transfer and particle deposition for oral breathing in a realistic human upper airway model. J. Therm. Biol. 70, 53–63.
Zhang, Z., Kleinstreuer, C., 2003. Species heat and mass transfer in a human upper airway model. Int. J. Heat Mass Transf. 46, 4755–4768.